The EMBO Journal Vol.16 No.3 pp.599–610, 1997

Viroid processing: switch from cleavage to ligation is driven by a change from a tetraloop to a loop E conformation

Tilman Baumstark, Astrid R.W.Schröder and Detlev Riesner[1]

Institut für Physikalische Biologie, Heinrich-Heine-Universität Düsseldorf, Universitätsstrasse 1, 40225 Düsseldorf, Germany

[1]Corresponding author

A longer-than-unit-length transcript of potato spindle tuber viroid is correctly processed in a potato nuclear extract only if the central conserved region is folded into a multi-helix junction containing at least one GNRA tetraloop–hairpin. The cleavage–ligation site between G^{95} and G^{96} was mapped with S1 nuclease and primer extension. The structural motifs involved in the processing mechanism were analysed by UV crosslinking, chemical mapping, phylogenetic comparison and thermodynamic calculations. For processing, the first cleavage occurs within the stem of the GNRA tetraloop; a local conformational change switches the tetraloop motif into a loop E motif, stabilizing a base-paired 5′ end. The second cleavage yields unit-length linear intermediates, whose 3′ end is also base-paired and most probably coaxially stacked in optimum juxtaposition to the 5′ end. They are ligated to mature circles autocatalytically, with low efficiency, or enzymatically, with high efficiency.

Keywords: chemical mapping/cleavage–ligation site/processing extract/RNA structure calculation/UV crosslinking

Introduction

Viroids are plant pathogens distinguished from viruses by the absence of a protein coat and by their small size. They are circular, single-standed RNA molecules consisting of a few hundred, generally 240–600, nucleotides. Native viroids adopt an unbranched, rod-like secondary structure with a high degree of intramolecular base-pairing (Gross *et al*., 1978). There is no evidence for any viroid-encoded translation product. Thus, viroid replication and pathogenesis entirely depend on the host enzyme systems (for reviews, see Riesner and Gross, 1985; Diener, 1987; Semancik, 1987; Symons, 1990). Current models of viroid replication assume different types of rolling circle mechanisms (reviewed by Branch and Robertson, 1984; Sänger, 1987; Daròs *et al*., 1994). As the final step the oligomeric (+) strand RNA has to be cleaved to unit-length molecules, which are then ligated to the mature viroid circles. Two special viroids, ASBVd and PLMVd, contain the hammerhead-ribozyme sequences (Forster and Symons, 1987) and self-cleave *in vitro* (Hutchins *et al*., 1986; Hernández and Flores, 1992). For all other viroids self-cleavage could not be shown in spite of repeated attempts (see for example, Tsagris *et al*., 1987). Nevertheless, the protein-dependent mechanism of viroid processing also requires particular structural features that are responsible for specific interactions with host cleavage and ligation enzymes. A large group of viroids, including the potato spindle tuber viroid (PSTVd), share a region of high homology in the central part of the rod-like structure, the so-called central conserved region (CCR). Linear RNA transcripts with a short terminal duplication in the upper part of the CCR were shown to be highly infectious (Tabler and Sänger, 1984; Meshi *et al*., 1985; Candresse *et al*., 1990; Rakowski and Symons, 1994). From these results it was concluded that the processing of viroids proceeds within this region (Hashimoto and Machida, 1985; Diener, 1986; Steger *et al*., 1986; Hecker *et al*., 1988). Therefore PSTVd-specific constructs of this kind can be regarded as model RNAs for the natural replication intermediates and it has been shown that they can adopt quite different conformations (Steger *et al*., 1992). The secondary structures of a longer-than-unit-length transcript used in the present study have been analysed recently (Baumstark and Riesner, 1995). Single conformations could be established in solution by well-defined buffer and temperature treatments; a subset of structures, i.e. those of interest for the present work, are depicted in Figure 1. Either the 5′ or the 3′ segment of the duplication or parts of both protrude from the otherwise unperturbed, rod-like secondary structure. Only one of these structures (ExM in Figure 1) was accurately processed to mature circular products upon incubation with a nuclear extract from the host plant potato. Since the active and inactive conformations of the substrate RNA share most of the extended, i.e. rod-like structure, it is obvious that local differences, in fact within the CCR, determine the substrate activity for correct cleavage and ligation.

In this work the cleavage and ligation sites within the substrate RNA were identified. They were found close to a region with a high sequential and structural homology to the loop E of 5S rRNA. The spatial arrangement of the bases in the loop E motif, in PSTVd as well as in 5S rRNA, was known from a UV-induced interstrand crosslink (Branch *et al*., 1985). In an attempt to confirm this local structural element, we found it clearly present in the linear and circular products of viroid processing, but not in the active conformation of the substrate. According to the secondary structure model of the active conformation, however, a UV-induced crosslink would have been expected. Refined analysis, also including chemical mapping, revealed that the region including the loop E element can be rearranged into a structural alternative by formation of two hairpins, one with a tetraloop of the GNRA type. In viroids of the PSTVd class the possibility for formation of this tetraloop is strictly conserved. We present a mechanistic model of viroid processing, in which

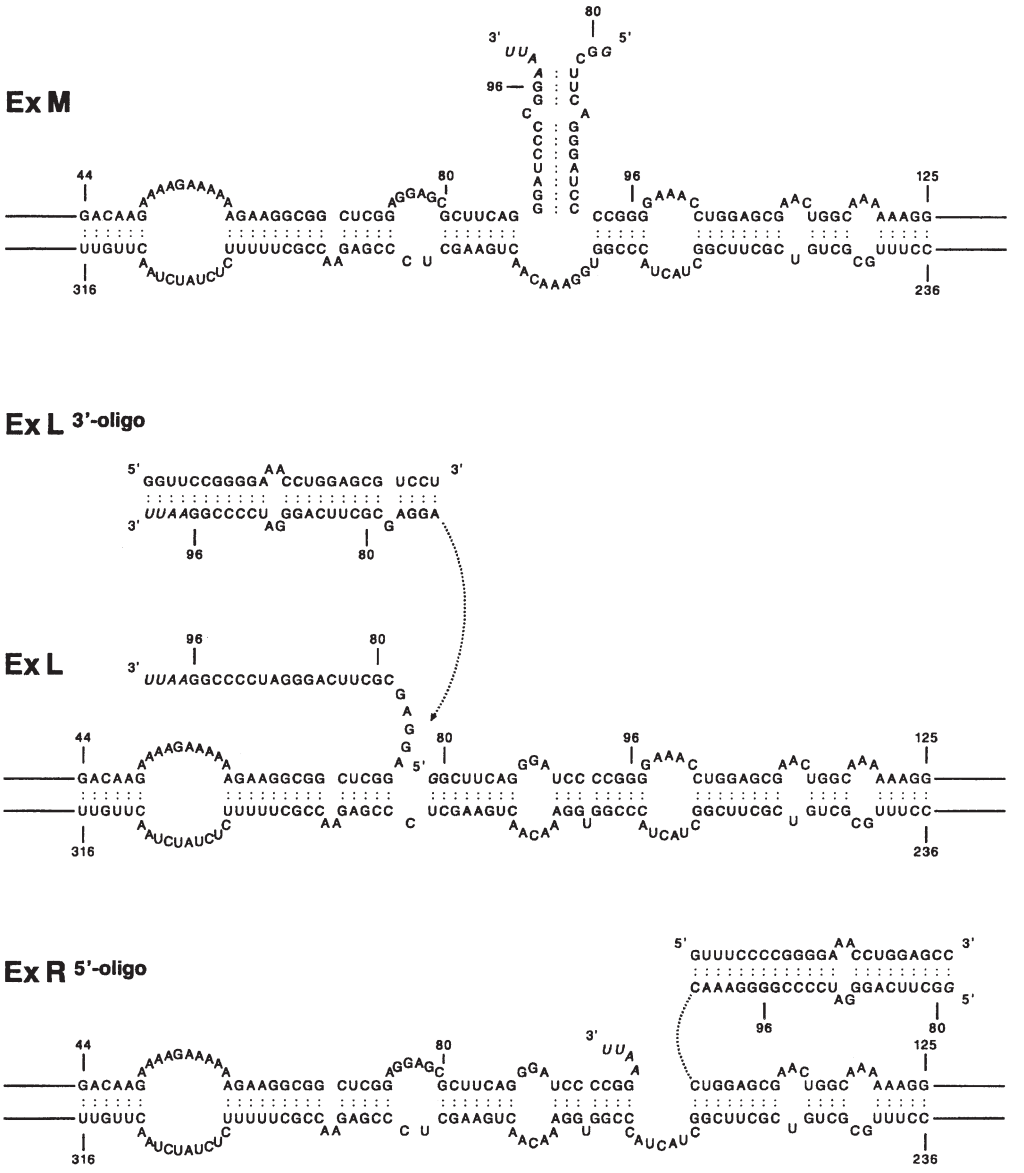

Fig. 1. The longer-than-unit-length transcript TB110 in different conformations as published earlier (Baumstark and Riesner, 1995). The conformations differ only in the central part of the characteristic rod-like structure of viroids; the terminal parts are identical to circular PSTVd in all cases shown and are therefore represented by straight lines left and right. The extended middle (ExM) extended left (ExL) and extended right structure ($ExR^{5'\text{-oligo}}$) are named according to the position of the segments branching out from the native rod-like structure. The extended right structure is stable only as a hybrid with the complementary 5′-oligonucleotide; in analogy, the hybrid $ExL^{3'\text{-oligo}}$ can be formed by annealing with the complementary 3′-oligonucleotide. Nucleotides G^{80} and G^{96} (all numbering of sequences refers of Gross *et al*., 1978) mark the first and last base of the sequence duplication at the 5′ or 3′ end of transcript TB110, respectively; vector-derived nucleotides of transcript TB110 are given in italics. In $ExL^{3'\text{-oligo}}$ and $ExL^{5'\text{-oligo}}$, respectively, one phosphodiester bond had to be enlarged for graphic reasons (dashed lines).

the tetraloop substructure specifies the first cleavage, followed by a conformational change into a loop E-containing structure responsible for the second cleavage and the ligation.

Results

Processing reactions in the nuclear extract

The PSTVd-specific transcript TB110 of longer-than-unit length (381 nt) was used as substrate for processing in the potato nuclear extract. The active substrate conformation ExM was established as described earlier (Baumstark and Riesner, 1995). This transcript, abbreviated L_0 in this report when used as a substrate, yields linear intermediates L_1 and L_2 of shorter length (Figure 2, left panel) as well as circular products (right panel, lane L_0, E) upon incubation with the nuclear extract. When the linear intermediates L_1 and L_2 were eluted from the gel according to standard procedures (Krupp, 1988) and reincubated with the nuclear extract, correct circles of 359 nt length (C_{359}) were produced (Figure 2, right panel, lanes L_1, E and L_2, E). This behaviour is consistent with the assignment of L_1 and L_2 as intermediates of the processing pathway. Incubation of substrate L_0 and intermediate L_1 (Figure 2, lanes L_0, Ø and L_1, Ø) in processing buffer including Mg^{2+} and the nuclear extract's storage buffer without proteins (lanes L_0, B and L_1, B) did not result in detectable amounts of correct circular molecules C_{359}. In contrast,

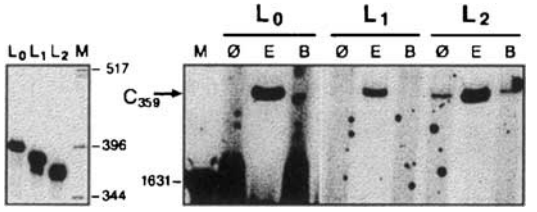

Fig. 2. Analysis of linear and circular products of the processing reaction. Radiolabelled longer-than-unit-length transcript TB110 as substrate L_0 (cf. Figures 1 and 3D) was incubated with the nuclear extract (Baumstark and Riesner, 1995). Substrate L_0 as well as the resulting processing intermediates L_1 and L_2 were eluted from a 5% PAA denaturing gel and re-analysed (left panel). A total of 10^5 c.p.m. was either reincubated with nuclear extract (right panel, lanes E), incubated in processing buffer (lanes B) or kept untreated (lanes Ø) and was then analysed for the formation of correct circular products (C_{359}, arrow) on a 5% PAA denaturing gel. Lanes M, pBR 322/*Hin*fI.

we found a significant amount of C_{359} directly after elution of intermediates L_2 from the gel (lane L_2, Ø); the yield was not further enhanced by incubation in the protein-free processing buffer (lane L_2, B). Since L_2 was identified as the exact monomeric unit of 359 nt (see below), the circles C_{359} in lane L_2, Ø must be a product of autoligation of L_2 during the overnight elution from the gel. Whereas autoligation has been shown for self-cleaving plant viral satellites (Buzayan *et al*., 1986; Etscheid *et al*., 1995) and for *in vitro* transcripts of PLMVd after self-cleavage and subsequent folding into the rod-like structure (Lafontaine *et al*., 1995), it has not to date been observed for any other viroid. In the presence of nuclear proteins (lane L_2, E); however, ligation was more efficient by at least a factor of 10. This implies that autoligation might be rather relevant with respect to the evolution of the viroid replication cycle than for the mechanism of processing in the present host plant system.

Determination of cleavage and ligation sites

The sites of enzymatic cleavage and ligation were determined by mapping the 5′ and 3′ ends of the linear intermediates. For mapping of the 3′ ends, L_1 and L_2 were hybridized with a labelled complementary DNA strand as described in Materials and methods. After incubation with nuclease S1 the exact length of the DNA probe protected against degradation by the RNA's 3′ end was determined on denaturing gels in comparison with a sequencing ladder. As shown in Figure 3A, the intermediates L_1 and L_2 bear a 3′ end with G^{95} as the last nucleotide; the position of this 3′ cleavage site in respect to the duplicated sequence of the longer-than-unit-length substrate is indicated in Figure 3D.

Mapping of the 5′ ends by primer extension revealed that G^{95} is the first 5′ nucleotide of the processing intermediates L_2 (Figure 3B), whereas intermediates L_1 showed the same 5′ end as the substrate transcript L_0 or one nucleotide shorter, which could not be differentiated experimentally (data not shown). While this identifies L_2 unequivocally as the linear intermediate of exact monomeric unit length having been cleaved twice at the same relative position between nucleotides G^{95} and G^{96} (Figure 3D, filled arrowheads), the nature of the 5′ end of L_1 remained unclear at this point. To investigate the possibility that L_1 could be an intermediate of the larger circular RNA species, which appeared as aberrant products of the processing reaction (Baumstark and Riesner, 1995; cf. also Figure 4A, C_a), these aberrant circles C_a were analysed by PCR amplification and subsequent direct DNA sequencing. As shown in Figure 3C, C_a is longer than C_{359} by a stretch of 16 nt, incorporating most of the duplicated PSTVd sequence of the transcript used as substrate L_0. The aberrant circles can easily be interpreted as premature ligation products of L_1, if its 5′ end was one nucleotide shorter than the substrate transcript. If, however, a second 5′ cleavage occurs after G^{95} before ligation, the correct circles are produced (cf. right panel of Figure 2, lane L_1, E).

Characterization of the RNA recognition motifs for cleavage and ligation

Figure 4 describes the relationship between conformation, conformational transition and processing activity of the substrate transcript L_0. As reported earlier (Baumstark and Riesner, 1995) and reproduced clearly in Figure 4A, conformation ExM (cf. Figure 1) was the only conformation yielding high levels of correct circles C_{359}, whereas the alternative conformation ExL (cf. Figure 1) yielded mainly aberrant circles C_a of larger size and only marginal amounts of correct circles. The active structure ExM, however, is metastable under salt and temperature conditions of the processing reaction and undergoes a conformational transition into the inactive structure ExL: in the absence of nuclear extract proteins ExM had virtually disappeared after 15 min of incubation (Figure 4B). On the other hand, the kinetics of product formation from substrate L_0 preformed into structure ExM shows that a major portion of correct circles C_{359} are produced between 15 and 30 min incubation time with the nuclear extract (Figure 4A). Obviously the nuclear extract proteins, which perform the processing reaction, stabilize structure ExM against transition into conformation ExL. Both observations, the stabilization of ExM as well as its substrate activity, led to the working hypothesis that specific structural motifs displayed by the RNA in conformation ExM but not in ExL are recognized by the proteins involved in the processing reaction. Consistently, it is most reasonable to assume that such a recognition motif would include or be positioned close to the actual cleavage sites.

In fact, the cleavage site between G^{95} and G^{96} is located within the CCR, only one base-pair apart from a large loop (positions 97–102 and 256–262), which exhibits a remarkable homology to the loop E in eukaryotic 5S rRNA (Branch *et al*., 1985). Furthermore, it is similar to the α-Sarcin-sensitive loop in 28S and 23S rRNA (see Gutell *et al*., 1992) and the loop B in the hairpin ribozyme from the tobacco ringspot virus-associated satellite RNA (Butcher and Burke, 1994a). Biochemical studies on loop B and NMR studies on model oligonucleotides have revealed a complex pattern of Watson–Crick and non-canonical base-pairs (Wimberly *et al*., 1993; Butcher and Burke, 1994b; Szewczak and Moore, 1995). Branch and colleagues deduced the loop E-like motif in viroids from a characteristic UV crosslink between the two bases G^{98} and U^{260} located in opposite strands of the CCR (Branch *et al*., 1985; Paul *et al*., 1992).

We used this crosslink as a tool to assess the presence of loop E in the substrate RNA after establishing the

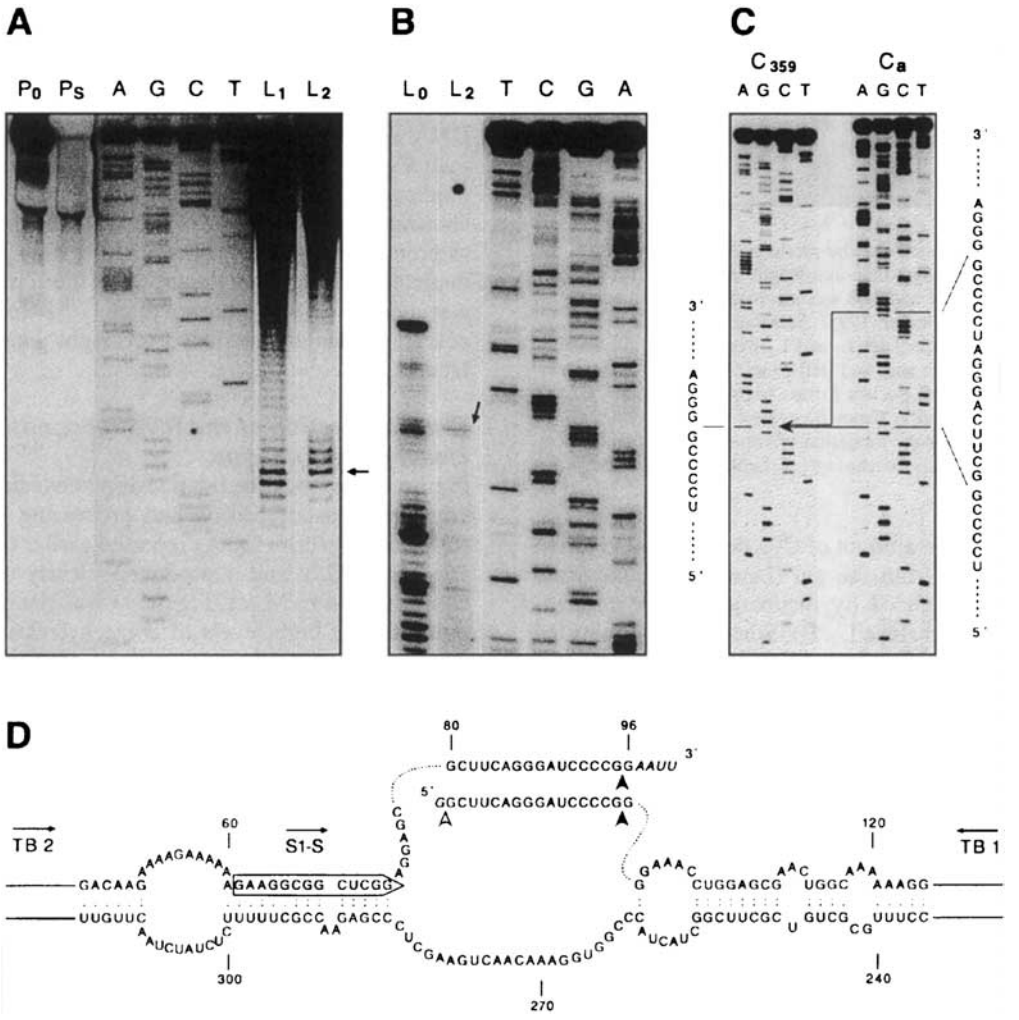

Fig. 3. Determination of 5′- and 3′-cleavage and ligation sites. (**A**) 3′ ends of linear intermediates, analysed by nuclease S1 protection. (**B**) 5′ ends of intermediates L_2, analysed by primer extension. (**C**) Sequence of aberrant and correct circular processing products, obtained after RT–PCR amplification. (**D**) Representation of the substrate transcript L_0 including cleavage sites and position of primers. (A) Linear intermediates L_1 and L_2, respectively, were annealed with labelled ssDNA probe of (−) polarity, incubated with S1 nuclease and the S1-resistant material was analysed on an 18% PAA denaturing gel. Lanes A, G, C and T, sequencing reaction of unlabelled PCR fragment S1-S/TB1 with 5′-labelled primer S1-S according to published protocols (Petersen *et al*., 1994); lanes L_1 and L_2, S1-resistant samples of the respective linear intermediates; lane P_S, control samples treated without protecting RNA; lane P_0, control samples treated without nuclease S1. The band corresponding to the 3′-G^{95} (lanes L_1, L_2) is denoted by an arrow. (B) Primer extension products of substrate L_0 and intermediate L_2 were analysed on an 8% PAA denaturing gel. Lanes T, C, G and A, sequencing reaction of the TB1/S1-S PCR product with unlabelled primer TB1 and [α-^{32}P]dCTP (Petersen *et al*., 1994). The band corresponding to the 5′-G^{96} (lane L_2) is denoted by an arrow. (C) Lanes A, G, C and T, sequencing reactions analysed on a 12% PAA denaturing gel. The sequence duplication present in C_a (right side of the panel) in comparison with C_{359} (left side) is reproduced in detail as an insertion on the right side and marked as an arrowed bracket within the autoradiograph. (D) The central section of the substrate transcript in its extended conformation. The 5′ and 3′ sequences are drawn in parallel as single strands to show the duplication (nt 80–96 as indicated); numbering of the PSTVd-specific nucleotides refers to Gross *et al*. (1978). The correct and aberrant cleavage sites are denoted by filled or open arrowheads, respectively. Primers TB1 and TB2 are located outside the reproduced section near the terminal ends of the viroid rod symbolized by straight lines. The position of primer S1-S is marked by the boxed sequence. Vector-derived nucleotides on the 5′ and 3′ end are given in italics.

different structures depicted in Figure 1. Beside the processing structure ExM and the structure ExL a structure $ExL^{3'OL}$ was established, in which the protruding 3′ segment of the duplication is stabilized by hybridization with a complementary oligonucleotide. Correspondingly, the protruding 5′ segment is hybridized to a respective complementary oligonucleotide in the conformation $ExR^{5'OL}$. After UV irradiation and analysis in denaturing gels, five or six crosslinked species were identified by their characteristic retardation (Figure 5A). Primer extension analysis of both upper and lower strand of the rod-like secondary structure revealed that the most prominent retarded band (open arrowhead in $ExL^{3'OL}$ and ExL) maps to the loop E-specific crosslink X^E (data not shown). Quantification of the crosslinking efficiency by phosphorimaging showed that up to 12% of the RNA applied to UV irradiation could be transformed into the crosslinked species X^E (data not shown). An alternative crosslinked band, resulting mainly after irradiation of structures ExM and $ExR^{5'OL}$ (Figure 5A, asterisk), accumulated to a much lesser extent, i.e. <0.3% of the total RNA applied (data not shown) and could therefore not be recovered in amounts sufficient for primer extension analysis. The appearance of band X^E indicating the presence of loop E in structures $ExL^{3'OL}$ and ExL, which were inactive in the processing reaction, and its absence in $ExR^{5'OL}$ is in

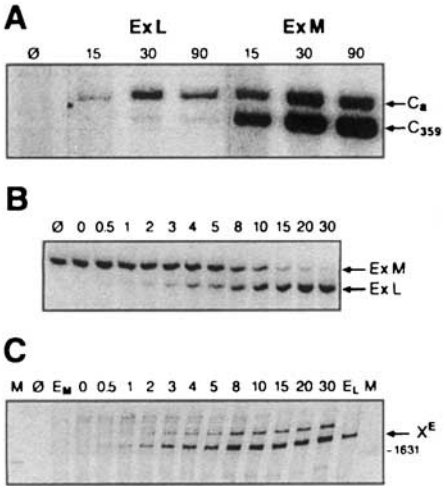

Fig. 4. Kinetics of enzymatic formation of circular processing products from substrate L_0 in structures ExL and ExM (**A**) in comparison with the conformational transition from structure ExM to ExL in processing buffer without proteins (**B** and **C**). (A) Labelled substrate transcript L_0 (10^5 c.p.m.) was pretreated to either fold into structure ExL or ExM (Baumstark and Riesner, 1995), incubated with the processing extract for the times indicated and analysed by 5% PAA denaturing gel electrophoresis for circular processing products. Lanes 15, 30 and 90, incubation times in min; lane Ø, unprocessed control. C_a, aberrant, C_{359}: correct circular products. (B) Labelled substrate L_0 was pretreated by low salt snap cooling to fold into the active structure ExM, incubated at 30°C in processing buffer including 10 mM Mg^{2+} for the times indicated, chilled on ethanol/ice, dialysed against TE buffer at 4°C and analysed on a 5% PAA non-denaturing gel at 15°C. Lanes 0–30, incubation times in min; lane Ø, neither incubation nor dialysis. Structures ExM and ExL are denoted by arrows. (C) Labelled substrate L_0 was pretreated to fold into ExM conformation [cf. (B)], incubated in processing buffer for times indicated in 10 μl aliquots and transferred to ethanol/ice. The samples were exposed to UV irradiation for 30 min on ice and analysed on a 5% PAA denaturing gel for retarded, crosslinked RNA species. Lanes 0–30, incubation times in min; lanes E_M and E_L, preformed structures ExM and ExL were UV-irradiated in TE instead of processing buffer without prior shift to 30°C; lane Ø, UV-untreated transcript; lane M, pBR 322/*Hin*fI. X^E, loop E-specific crosslink as determined by primer extension (data not shown).

accordance with the proposed secondary structure models (Baumstark and Riesner, 1995; cf. also Figure 1). The absence of the loop E-specific crosslink X^E in the active structure ExM, however, is clearly at variance with the structural model given in Figure 1.

Investigating local conformational alternatives to the loop E in the active substrate we performed secondary structure calculations with the program LinAll (Schmitz and Steger, 1992) using a recent thermodynamic parameter set, which includes parameters for tetraloops (Groebe and Uhlenbeck, 1988; Antao *et al*., 1991; Antao and Tinoco, 1992). The structure ExM containing the loop E motif (Figure 6, ExM^E) was predicted with lowest free energy, i.e. a ΔG^0 of −434.5 kJ/mol, even after including tetraloop parameters. The rod-like structure ExL comprising loop E (Figure 6, ExL) was predicted as suboptimal with a ΔG^0 of −414.4 kJ/mol. Searching for suboptimal structures without loop E, we introduced the restraint that one of the loop E flanking base-pairs, i.e. either G^{97}:C^{262} or C^{103}:G^{255}, are prohibited within the calculation; by this procedure a new folding pattern was obtained, which is shown in Figure 6 (ExM^{TL}). The upper strand folds into a GAAA tetraloop closed by a G:C-rich stem (nucleotides 93–106) and the lower strand forms a small regular hairpin loop. Additionally, another GAAA tetraloop can be formed in the lower strand. This conformation ExM^{TL} has a ΔG^0 of −403.3 kJ/mol, when the second tetraloop in the lower strand is present (as depicted) and a ΔG^0 of −410.1 kJ/mol without the second tetraloop. The phylogenetic, kinetic and tertiary structure arguments in favour of the second tetraloop will be discussed later.

Since UV crosslinking was performed in low salt buffer without Mg^{2+}, it might be argued that in the presence of Mg^{2+} the active substrate ExM assumes the loop E instead of the tetraloop motif in contrast to our results described above. Therefore, the structural information obtained at low salt had to be confirmed for the buffer conditions of the processing reaction, which include 10 mM Mg^{2+}. For such an analysis the transcript in conformation ExM was incubated at 30°C in processing buffer, including Mg^{2+} for increasing time and then tested for loop E-specific UV crosslinking. This kinetics of loop E formation, shown in Figure 4C, was compared with the kinetics of the conformational rearrangement from ExM to ExL under identical conditions (Figure 4B). At 0°C and without preincubation at 30°C the loop E-specific crosslink X^E is barely detectable in TE buffer (Figure 4C, lane E_M) as well as in processing buffer (lane 0). This demonstrates that the presence of Mg^{2+} alone does not promote a conformational change from the tetraloop to the loop E structure. The consecutive accumulation of the loop E-specific crosslink with prolonged preincubation under conditions of the processing buffer at 30°C (Figure 4C, lanes 0.5–30) reveals the same kinetics as the ExM to ExL transition (Figure 4B, lanes 0.5–30). The final yield of crosslinked loop E is significantly higher in the presence (Figure 4C, lane 30) than in the absence of Mg^{2+} (lane E_L), indicating a specific binding of Mg^{2+} to the loop E region. Furthermore, an additional UV-crosslinked species of low concentration emerges in parallel to ExL formation, which was not observed in the absence of Mg^{2+} (lane E_L). We conclude from these experiments that the tetraloop motif in the active substrate ExM^{TL} does not switch into a loop E conformation ExM^E with rapid kinetics and then slowly refolds into structure ExL, but rather that the loop E motif appears exclusively as an element of ExL.

To verify the predicted tetraloop conformation for the active processing structure ExM in contrast to the loop E-containing structure, ExL, we performed structural analysis of ExM and of ExL by chemical modification of unpaired bases with dimethylsulfate (DMS) and subsequent primer extension (Figure 7). Sites of significant modification above the background of unmodified RNA (lanes Ø) that reproducibly differed between ExM and ExL in four to five independent experiments are denoted by arrows. It should be noted that modified nucleotides on the RNA result in a termination of the primer extension reaction at the base preceding the modification site. Therefore, the nucleotide responsible for a stop is one position up in the sequencing lanes from the primer extension stop itself. Our modification data strongly support the correlation of the tetraloop motif with structure ExM and the loop E with structure ExL as inferred from the results summarized in Figure 6. In particular, base C^{262}, which is involved in a stable G:C base-pair within the context of loop E (cf. Figure 6, ExL), was not accessible to DMS in structure

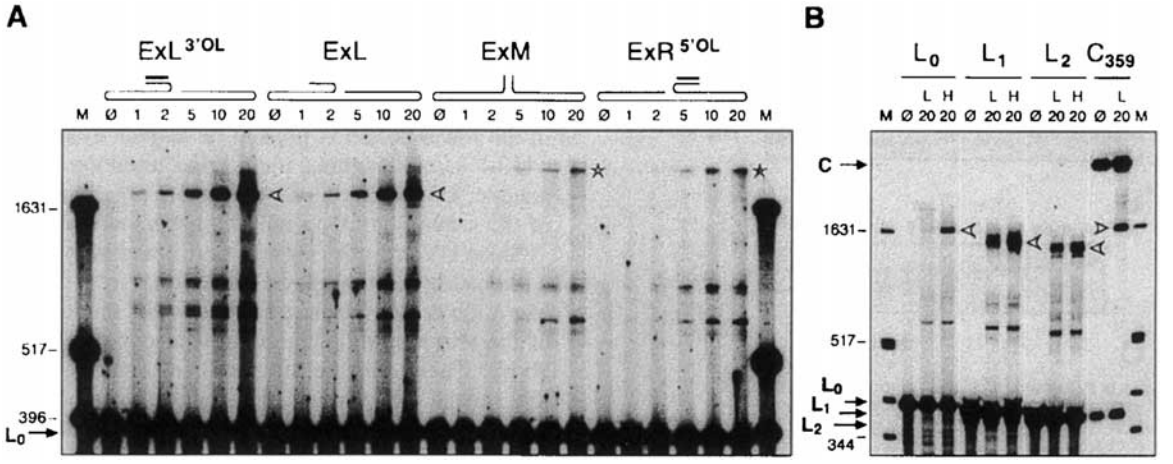

Fig. 5. Analysis of the formation of loop E in the substrate transcript present in four different secondary structures (**A**) and its comparison as substrate L_0 with the linear intermediates L_1 and L_2 and the circular product C_{359} of the processing reaction (**B**). The different conformations of the substrate transcript, the extended left structure with ($ExL^{3'OL}$) or without 3′-oligonucleotide (ExL), the extended middle structure (ExM) or the extended right structure with 5′-oligonucleotide ($ExR^{5'OL}$) (cf. Figure 1) were induced by corresponding pretreatments as published (Baumstark and Riesner, 1995); they are depicted schematically in the head of panel (A). Substrate L_0, gel-eluted L_1, L_2 and C_{359} were subjected to pretreatments in high salt or low salt buffer to establish the secondary structures ExL or ExM, respectively, in the substrate transcript L_0 (Baumstark and Riesner, 1995) as well as corresponding structures in the linear intermediates L_1 and L_2 or the circular products C_{359} in the experiment of panel (B). After dialysis in TE buffer at 4°C, samples were placed on ice-water, UV-irradiated for the times indicated and analysed on a 5% PAA denaturing gel. Lanes Ø–20, time of UV irradiation in min; lanes L and H, low salt or high salt pretreatment, respectively; lanes M, pBR 322/*Hin*fI. The bands of non-crosslinked RNA of substrate transcript (L_0), linear intermediates (L_1 and L_2) and circular product (C) are indicated by filled arrows; the loop E-specific UV crosslink X^E (open arrowheads) as well as the additional crosslink appearing with substrate structures ExM and $ExR^{5'OL}$ (asterisk; cf. text) are marked within the panels.

ExL (Figure 7B, lane ExL), whereas its modification in structure ExM (lane ExM) is in good accordance with the predicted regular hairpin loop in the lower strand of the tetraloop conformation (Figure 6, ExM^{TL}). Furthermore, base C^{102} is strongly accessible to DMS modification in structure ExL (Figure 7A, lane ExL) as it can be expected in a loop E conformation (Figure 6, ExL), while in contrast a pronounced protection of this base can be observed in structure ExM (Figure 7A, lane ExM). This is consistent with the presence of the tetraloop motif in the upper strand (Figure 6, ExM^{TL}). In addition, the correlation that C^{102} in the loop E-containing structure ExL is modified in decreasing amounts with increasing magnesium concentrations (data not shown) reveals exactly the same behaviour as the related loop B in the hairpin ribozyme at the homologous position (Butcher and Burke, 1994b); it thus further supports our observation that the loop E motif in ExL is stabilized by Mg^{2+}. The chemical modification of nucleotide A^{85} close to the 5′ end of the transcript cannot be interpreted in such a straightforward manner as compared with C^{102} and C^{262}, which are located in well-defined structural motifs. Nucleotide A^{85} is accessible in structure ExL and protected in ExM, whereas the opposite tendency would have been expected from the structures given in Figure 6. However, A^{85} is located in a much less characterized domain; unusual base-pairs and/or tertiary base contacts in structure ExM as well as early melting of the 5′ terminal helix in structure ExL might influence the modification in an (at present) unpredictable way.

The stem with a GNRA-type tetraloop as a new structural alternative within the CCR domain is supported by phylogenetic arguments. A sequence alignment of viroids from the PSTVd class including the most recently discovered Mexican papita viroid (MPVd) of putative ancestral origin (Martínez-Soriano *et al.*, 1996) is depicted for the upper and lower CCR in Figure 8. This alignment reveals a cluster of three or four conserved stems with tetraloops within the CCR or nearby, whereas only one more tetraloop with a lower degree of conservation was found in the remaining 250–300 nt of the viroid RNAs (not shown). Among the cluster of tetraloops, the stem with GAAA tetraloop shown in Figure 6 (ExM^{TL}) is absolutely conserved in all viroids of the PSTVd class. Exactly this tetraloop motif contains the cleavage site. Thus, the structural element containing the GAAA tetraloop is the best candidate for recognition by the host processing enzyme(s). In this context earlier structural models should be mentioned, which suggested an evolutionary relationship between viroids and introns (Diener, 1986, 1989; Dinter-Gottlieb, 1986); they deviated completely from the viroid rod-like structure, yet one contained the stem–tetraloop motif (Dinter-Gottlieb, 1986). Furthermore, this tetraloop hairpin is conserved among group I introns, as the so-called domain P5b/L5b, as well as among group II introns, where it was termed domain V (Michel and Dujon, 1983; Costa and Michel, 1995).

Structure of the processing intermediates

The structure of the linear intermediates L_1 and L_2 was also investigated using UV crosslinking. The linear intermediates L_1 and L_2 were transformed into defined structures by the same pretreatments as the substrate transcript L_0, i.e. under specific temperature and solution conditions (see Baumstark and Riesner, 1995), and analysed in comparison with substrate L_0 and the circular product C_{359} (Figure 5B). In contrast to Figure 5A, a single UV irradiation time was applied here. Lane L_0, L, i.e. low salt pretreatment and no significant crosslink formation, corresponds to ExM, and lane L_0, H, i.e. high salt pretreatment and marked formation of loop E-specific

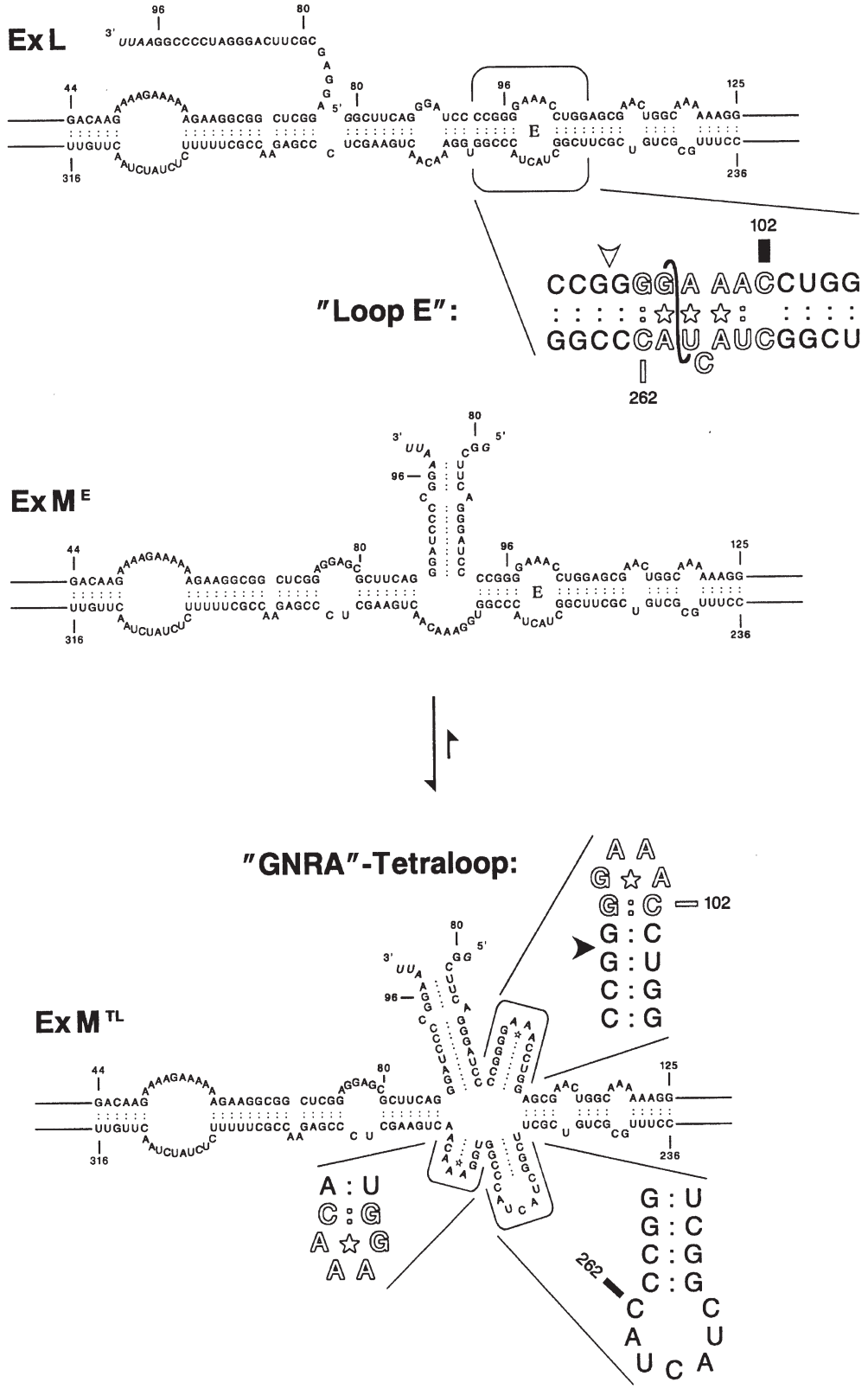

Fig. 6. The substrate transcript in secondary structure ExL and alternatives of structure ExM. Structure ExL and one conformation of structure ExM (ExM^E) contain loop E (see enlargement); the alternative ExM^{TL} comprises two tetraloops and a regular hairpin loop (see enlargements). Bases characteristic for the respective motif are given in outlined typeface, stars indicate non-canonical base-pairs, the S-shaped line connecting G^{98} and U^{260} in the enlargement of loop E denotes the loop E-specific UV crosslink (cf. Figure 5 and text). The site at which 5′-cleavage occurs if the substrate is in structure ExM, but not if it is in ExL, is denoted by a filled arrowhead in the upper tetraloop and by an open arrowhead in the loop E. The differences in DMS modification patterns of ExL and ExM shown in Figure 7 are denoted by rectangles designating the respective base in the loop E (for ExL) and the hairpins (for ExM); filled broad rectangles indicate strong accessibility, filled narrow rectangles moderate accessibility, and open rectangles protection against DMS modification.

crosslink, corresponds to ExL, thus clearly reproducing the characteristic behaviour of the RNA in its substrate state. In the linear intermediates L_1 and L_2, however, a strong UV-induced crosslink was obtained, regardless of the type of pretreatment (Figure 5B, lanes L_1 and L_2). Crosslinked species of L_1 and L_2 migrate faster than those of L_0 due to the shorter chain length as reflected by the same difference in mobilities of the unmodified RNA molecules (cf. L_0, L_1 and L_2 at the bottom of the gel). While the crosslinked RNAs of linear origin are retarded compared with the non-crosslinked species, the crosslinked circle is more compact and therefore migrates faster than the non-crosslinked circle (C in lanes C_{359}). The presence of linear molecules of the same monomeric length as L_2 in the preparation of C_{359} is due to random single-strand nicking of the circular product.

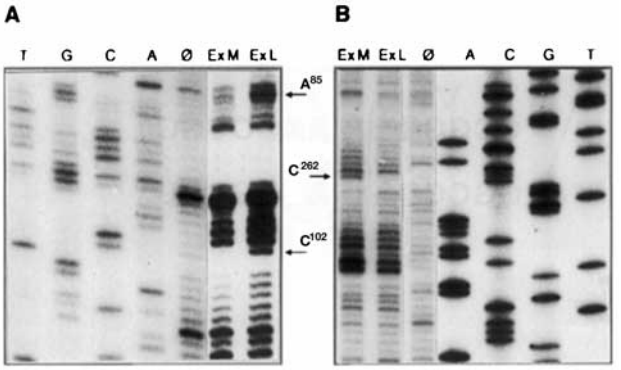

Fig. 7. DMS modification patterns of the substrate transcript in structures ExM and ExL. The transcript was pretreated to establish structures ExM or ExL (Baumstark and Riesner, 1995), treated with DMS (lanes ExM and ExL) or buffer (lanes Ø) and reverse-transcribed by primer extension; the modification sites were analysed on an 8% PAA denaturing gel in comparison with the viroid sequence in plasmid DNA (lanes A, C, G and T, respectively) and are designated by arrows and numbered nucleotides. (**A**) Analysis of the upper strand of the substrate transcript by primer extension with primer TB1 after 30 min DMS modification. (**B**) Analysis of the lower strand of the substrate transcript by primer extension with primer RGV2 after 15 min DMS modification. Reproduction is restricted to regions overlapping with the upper strand [panel (A), nt 85–114] and the lower strand [panel (B), nt 243–291] of the viroid central conserved region (cf. text).

From this behaviour and the observation that the overall relative intensity of this crosslinked band in L_1 and L_2 is similar to those characterized in the control experiments (lanes L_0, H and C_{359}, L) we conclude that in the intermediates L_1 and L_2 the loop E-specific crosslink was induced. Remarkably, removal of only five nucleotides at the 3′ cleavage site of substrate L_0 leads to a significant amount of loop E conformation in L_1 (lane L_1, L), which is not present in L_0 (lane L_0, L) under low salt conditions. The amount of loop E conformation can be further enhanced by high salt pretreatment, as it is evident from the intensity increase of the crosslinked band (lane L_1, H). The presence of a loop E crosslink in L_2 demonstrates the integrity of the loop E motif even after cleavage of 17 nucleotides at the 5′ site, leaving only one base-pair (G^{95}:C^{263}) bordering loop E at the ligation site.

Discussion

Physical features of the tetraloop motif

In vitro, the tetraloop-containing structure ExM is favoured over structure ExL without tetraloop by low salt snap-cooling of the denatured transcript (Baumstark and

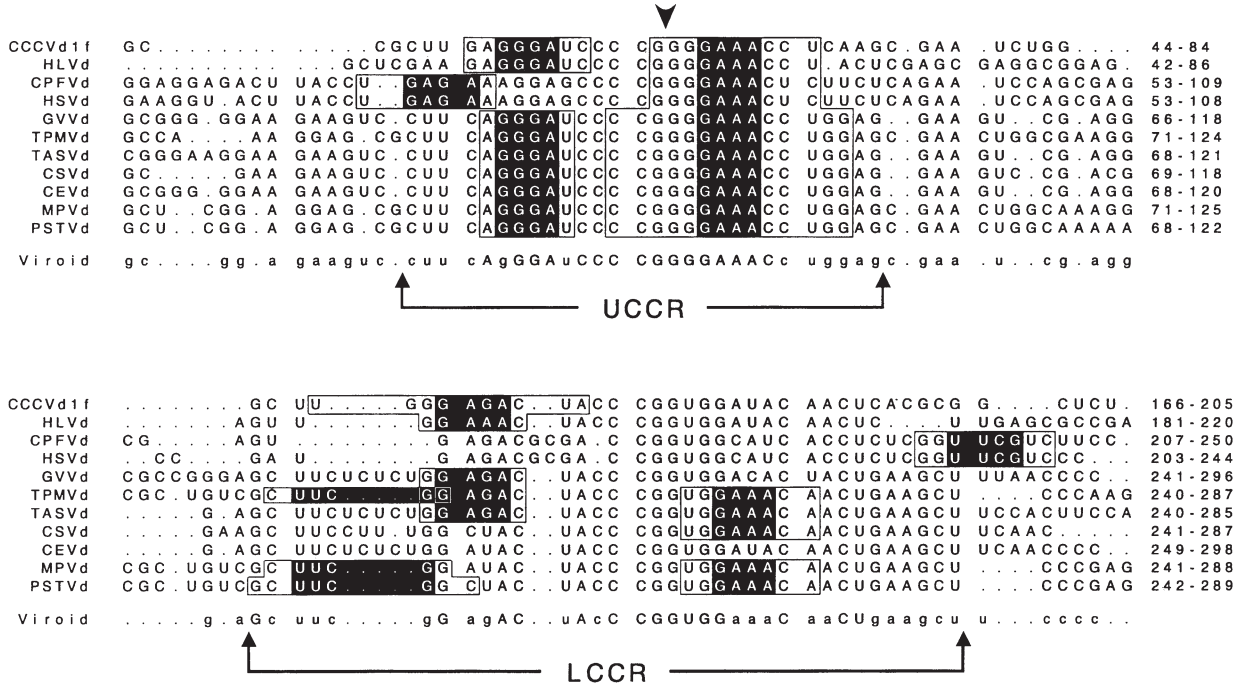

Fig. 8. Conservation of tetraloops within the central conserved region (CCR) of different viroids. Reproduction is restricted to the CCR and close neighbourhood of the PSTVd group; upper (UCCR) and lower strand (LCCR) of the CCR as parts of the viroid rod-shaped secondary structure are indicated. Tetraloop sequences are underlayed by black boxes, flanking bases able to form a base-paired stem are marked by open boxes; the cleavage site determined for PSTVd is marked by an arrowhead. In the consensus sequence (line viroid) a letter for a nucleotide is given if it appears in the alignment with a frequency of >50%; a capital letter represents a frequency of 100%. Numbers at the end of each line denote the first and last nucleotide of the respective viroid sequence referring to the entries in GenBank.

Riesner, 1995). Both properties, the advantage at low ionic strength as well as the fast structure formation must be expected for tetraloops. The independent formation of three hairpins, two with tetraloops, is faster than the serial formation of the different segments in the rod-like structure ExL. Since in a tetraloop at least three bases are stacked (for review, see Shen *et al*., 1995), the formation of the corresponding stem–loop structures has to be similarly fast or even faster as compared with the recombination of small hairpins, which was determined experimentally with times between 5 and 50 μs (for review, see Riesner and Römer, 1973). This kinetic advantage is not restricted to the *in vitro* structure formation by snap-cooling, but may be equally relevant during viroid replication *in vivo* by polymerase II, when the nascent oligomeric plus strands have to avoid stable, yet inactive structures and instead adopt crucial parts of the processing structure directly upon synthesis by sequential folding. Similar cases, where the regulation of RNA activity is controlled by the kinetics of structure formation have recently been investigated (Ma *et al*., 1994; Groeneveld *et al*., 1995). Also the low ionic strength conditions favour tetraloops over the extended rod-like structure. This can be derived from the dependence of the thermal stability upon the ionic strength, which is ⩽5°C per decade of Na^+ concentration change for small stem–loop structures (Coutts, 1971; Varani *et al*., 1991; Antao and Tinoco, 1992) compared with 13.2°C for the rod-like viroid structure (Langowski *et al*., 1978). The structural calculations predicting the loop E conformation to be favoured over the tetraloop conformation had to be carried out for 1 M ionic strength; therefore these calculations do not contradict our results at low ionic strength.

The model proposed for the tetraloop-containing structure consists of six helices emerging from one central loop with only one unpaired nucleotide (A^{261}). It is most likely not only stabilized by secondary structure interactions as represented in Figure 6 (ExM^{TL}), but also by contributions from tertiary structure. Coaxial stacking of helices as described for the tRNA-like 3′ end of brome mosaic virus genomic RNA (Felden *et al*., 1994) or for the distal protein-coding domains of RNA phage Qβ (Beekwilder *et al*., 1995) as well as tetraloop–tetraloop and tetraloop–helix interactions (Michel and Westhof, 1990; Jaeger *et al*., 1994; Murphy and Cech, 1994; Pley *et al*., 1994; Chanfreau and Jacquier, 1996) are well-known examples mediating higher-order RNA structure. Special attention should be given to the accumulating data concerning the three-dimensional structure of group I and group II introns, where both the GAAA tetraloop-capped domains (P5b/L5b and V, respectively) with homology to our tetraloop motif (cf. phylogenetic section in Results) are involved in tertiary interactions essential for the functional three-dimensional folding (Michel and Westhof, 1990; Murphy and Cech, 1994; Costa and Michel, 1995; Cate *et al*., 1996). In this respect the other tetraloops in the CCR, although less conserved in sequence and position (Figure 8), might still be important as structural elements in a complex three-dimensional structure.

Relevance of the tetraloop versus loop E motif antagonism for the pathway of viroid processing

Considering the features of the tetraloop containing structure ExM we propose a pathway for processing of PSTVd

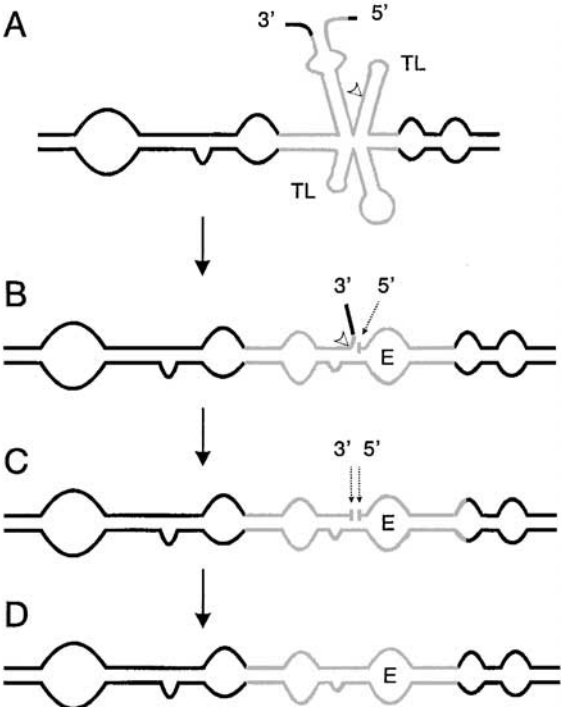

Fig. 9. Mechanistic model for viroid processing. The structures represent schematically the same central section from the complete viroid transcript as in Figures 1, 3D and 6. The sequences belonging to the CCR (refer to Figure 8) are given in grey. (**A**) The longer-than-unit-length RNA in tetraloop (marked TL) -containing conformation is substrate to the first cleavage (arrowhead; cf. also Figure 6, ExM^{TL}). (**B**) After dissociation of the short segment from the cleavage site, the newly generated 5′ end refolds and is stabilized by formation of loop E (denoted E), while the 3′ end is partially base-paired to the lower strand up to nucleotide G^{95}. The nucleotides at the 3′ end, which are left single stranded, are then cut off in the second cleavage step (arrowhead). (**C**) 5′ and 3′ end resulting from correct cleavage (broken arrows) are in juxtaposition stabilized by base-pairing and stacking. (**D**) Ligation of 5′ and 3′ end results in mature circular progeny.

(Figure 9). As a first step the tetraloop element in the structure ExM^{TL} is recognized by the host nuclease(s) and cleaved within the stem (Figure 9A). The 5′ fragment (nt 80–95) is released and the remaining CCR refolds into the rod-like secondary structure with the duplicated 3′ end left unpaired. Due to the helix-forming properties of loop E, which are enhanced by specific Mg^{2+} binding, the shortened 5′ end may be base-paired up to the terminal 5′-G^{96} (Figure 9B), thus replacing even 3′-G^{96}. This would explain the second cleavage occurring in the 3′ end between nucleotides G^{95} and G^{96}. In the resulting molecules of exact monomeric unit length 3′ and 5′ end are then placed in optimal juxtaposition, i.e. 3′-G^{95} and 5′-G^{96} are stacked onto each other coaxially (Figure 9C); such stacking interactions should not be regarded as static, but rather as a favourable state in a dynamic equilibrium. The ends may now be readily ligated to the mature circular product (Figure 9D) by a host plant RNA ligase; those enzymes have been described in other plant systems (Konarska *et al*., 1981; Branch *et al*., 1982; Kikuchi *et al*., 1982).

The existence of the 3′ cleaved intermediates L_1 does not contradict the proposed pathway. If the structure remains in the tetraloop conformation after an initial 3′ cleavage, consecutive 5′ cleavage, refolding and ligation

proceed unaltered. If, however, refolding into the loop E conformation occurs, which was observed in a substantial portion of L_1 (Figure 5B, lanes L_1, L and H), the 5′ recognition motif is lost and subsequent premature ligation would lead to the aberrant circles C_a.

The mechanism presented here is favoured by several features provided by all viroids of the PSTVd class. The recognition motifs for cleavage and ligation are unique in each monomeric unit of the oligomeric replication intermediate. Not only are they highly conserved among all viroids of the PSTVd class, but also the conformational changes can occur in all viroids of this class as they involve only the central conserved region (Figure 9, in red). The switch from the tetraloop structure to the loop E structure is nearly irreversible due to the dissociation of the 5′ cleavage fragment. Consequently, the conformational transition acts as a driving force from cleavage to the ligation reaction. The 3′ duplicated sequence can be cut off without specific recognition since it is the only segment protruding unpaired from the double helical region. The optimal juxtaposition of 5′ and 3′ end favours ligation, non-enzymatically with low efficiency, or enzymatically with higher efficiency. The importance of loop E is in accordance with results showing that adaptation of PSTVd from potato or tomato to the new host tobacco is accompanied by a single point mutation in loop E (Wassenegger *et al*., 1996). Finally, a covalently closed CCR in loop E conformation is no longer substrate to a backward cleavage reaction.

The processing mechanism of PSTVd as outlined in this work emphasizes the versatility of viroid structure. On one hand viroids have adopted an unusually stable structure to survive non-encapsidated within the host cell for a long time, while on the other hand they have evolved structural elements like G:C-rich stems (cf. Loss *et al*., 1991), loop E and tetraloops and thereby have acquired a high structural flexibility, enabling them to mimic different motifs for interaction with cellular factors.

Materials and methods

DNA oligonucleotides, plasmids and in vitro transcripts

Cloning of plasmid pTB110 used for generation of PSTVd-specific *in vitro* transcripts of more-than-unit length has been described previously (Baumstark and Riesner, 1995). In short, transcript TB110 consists of 381 nt, starting with a vector-derived G followed by PSTVd-specific sequence from nt 80–359/1–96 (numbering according to Gross *et al*., 1978) and again four vector-derived nucleotides AAUU. As DNA primers TB1 (nt 147–171, minus polarity), TB2 (nt 20–42, plus polarity), S1-S (nt 61–73, plus polarity) and RGV2 (nt 21–41, minus polarity) were used.

Buffers and processing with the nuclear extract

Processing reactions were performed by incubation of ^{32}P-labelled *in vitro* transcripts or gel-eluted linear intermediates with a nuclear extract derived from the host plant potato (Baumstark and Riesner, 1995) under conditions as indicated. For analysis of structural rearrangements of the substrate RNA occurring in parallel to the processing reaction as well as for autoligation reactions the nuclear extract was substituted with the buffer OSB (20 mM HEPES-KOH pH 7.9, 10 mM Mg-acetate, 50 mM K-acetate, 5 mM EDTA, 12 mM β-mercaptoethanol, 25% glycerol) used for preparation and storage; the finally resulting processing buffer includes 0.2 × OSB and, in addition to the components therein. 50 mM HEPES-KOH pH 7.9, 5 mM DTT and 8 mM $MgCl_2$. For renaturation of RNA in high ionic strength buffer 500/4/1/0.1 (500 mM NaCl, 4 M urea, 1 mM Na-cacodylate, 0.1 mM EDTA pH 7.9) or in low ionic strength TE (10 mM Tris-HCI pH 8.0, 1 mM EDTA), respectively, were used.

S1-mapping of processing intermediates' 3′ ends

A DNA probe was synthesized by PCR amplification of a plasmid containing a monomeric PSTVd-specific insert from nucleotides 282–1/359–281. By PCR with primers TB1 and S1-S in the presence of [α-^{32}P]dCTP and [α-^{32}P]dATP both strands of the resulting DNA fragment were labelled with high specific activity. The (−) strand was identified by SSCP-TGGE (Chen *et al*., 1995) in comparison with a PCR fragment labelled solely by incorporation of 5′-labelled primer TB1 of (−)-polarity and was then isolated by elution from a preparative SSCP gel. The resulting 111 nt ssDNA probe is complementary to any given TB110-derived 3′ sequence between PSTVd nt 61 and nt 96, thus exceeding the 3′ end of the longer-than-unit-length transcript used as substrate L_0 by 76 nt.

Linear intermediates L_1 and L_2, respectively, were annealed with 10^5 c.p.m. ssDNA probe prepared as above in a 10 µl volume containing 400 mM NaCl, 40 mM PIPES pH 6.4, 1 mM EDTA and 50% formamide by denaturation at 90°C and fast transfer to 37°C for overnight incubation (Casey and Davidson, 1977; Berk and Sharp, 1978). The samples were cooled on ice, 100 µl of ice-cold nuclease mix [250 mM NaCl, 40 mM NaOAc pH 5.5, 1 mM $ZnCl_2$, 10 µg/ml freshly denatured and chilled ctDNA and 200 U of nuclease S1 (BRL)] were added and incubation was carried out for 90 min at 15°C. The reaction was stopped by addition of 30 µl stop-mix [4 M NH_4OAc, 50 mM EDTA pH 8.0, 100 µg/ml tRNA (Boehringer)]. The S1-resistant material was precipitated with 3 volumes of ethanol:acetone (1:1), redissolved in urea loading solution and denatured before electrophoretic analysis on 18% PAA denaturing gels.

Primer extension analysis of processing intermediates' 5′ ends

RNA was annealed with 2.5×10^5 c.p.m. labelled primer TB1 in 30 µl buffer (100 mM NaCl, 50 mM Tris-HCl pH 8.3, 1 mM EDTA) by 5 min denaturation at 90°C and slow renaturation to room temperature overnight. Ethanol-precipatated pellets were redissolved and the RNA was transcribed into cDNA for 1 h at 48°C in 20 µl first strand buffer (BRL) in the presence of 500 µM dNTP, 10 mM dDTT, 20 U recombinant RNase inhibitor (RNasin, Promega) and 200 U reverse transcriptase Superscript II (BRL). The reaction was stopped by a 5 min incubation at 90°C, transfer of the samples to ice and ethanol/NH_4OAc precipitation. The RT products were redissolved in urea loading solution and denatured before electrophoretic analysis on 8% PAA denaturing gels.

RT-PCR sequencing of circular RNA processing products

Correct (C_{359}) and aberrant (C_a) circular products from a standard processing reaction of transcript TB110 as substrate L_0 with the nuclear extract were gel-eluted and amplified by RT-PCR with primers TB1 and TB2 as published (Baumstark and Riesner, 1995). The resulting PCR fragments were re-amplified with primers TB1 and S1-S, sequenced with 7.8×10^5 c.p.m. labelled primer S1-S (Petersen *et al*., 1994) and analysed on 12% PAA denaturing gels.

Secondary structure calculations

The calculation of RNA secondary structures and structural transitions was carried out on Alpha-AXP 3000/800 (Digital Equipment) using the algorithm LinALL (Schmitz and Steger, 1992) with additional implementation of thermodynamic parameters for tetraloop formation (Groebe and Uhlenbeck, 1988; Antao *et al*., 1991; Antao and Tinoco, 1992). ΔG^0-values are obtained for 1 M ionic strength, 1 M of each RNA species and refer to a calculation performed for a temperature of 40°C. RT-PCR primers were chosen according to calculations using a program developed recently (Steger, 1994).

UV crosslinking

RNA samples of $1–4 \times 10^4$ c.p.m. in 8 µl volume of TE or OSB buffer were placed in Eppendorf tubes on ice and were UV-irradiated at 258 nm wavelength for the times indicated using a stratalinker (model 1800, Stratagene). Subsequently, the RNA was either ethanol-precipitated, redissolved in urea loading solution and analysed on 5% PAA denaturing gels, or 4 µl loading solution were added to half the sample volume and applied directly to the gel.

DMS modification analysis

500 ng of the substrate transcript were pretreated to adopt the structure ExL or ExM, respectively (Baumstark and Riesner, 1995). Chemical modifications were carried out in a 200 µl volume containing 50 mM HEPES-KOH pH 8.0, 1 mM EDTA, 7 µg tRNA and 0.1% DMS for 15 and 30 min on ice. The reaction was stopped by addition of 14 µg carrier tRNA and ethanol precipitation, which was repeated once after

resuspending the pellet. Modification sites were identified by primer extension of 50 ng modified RNA with labelled primers TB1 and RGV2 at 52°C as described above. For reference, a plasmid containing viroid DNA was sequenced by the dideoxynucleotide chain termination method using Sequenase 2.0 (USB).

Alignment of viroid sequences

Sequences of viroids belonging to the PSTVd class were obtained from GenBank under the following accession numbers: cadang-cadang coconut viroid RNA 1 fast (CCCVd1f), J02050; hop latent viroid (HLVd), X07397; cucumber pale fruit viroid (CPFVd), X00524; hop stunt viroid (HSVd), X00009; grapevine viroid (GVVd), Y00328; tomato planta macho viroid (TPMVd), K00817; tomato apical stunt viroid (TASVd), K00818; chrysanthemum stunt viroid (CSVd), J02067; citrus exocortis viroid (CEVd), J02053; potato spindle tuber viroid (PSTVd), strain KF440-2, X58388. The sequence of Mexican papita viroid (MPVd) isolate OG1 was used as published (Martínez-Soriano *et al*., 1996); its accession number will be L78454. An alignment by the GCG program 'PileUp' with complete sequences was refined manually, taking into account results from alignments carried out earlier (Riesner and Steger, 1990).

Acknowledgements

We gratefully acknowledge Drs P.Klaff, M.Schmitz and G.Steger for critical reading of the manuscript and numerous stimulating discussions. The work was supported by grants from the Deutsche Forschungsgemeinschaft and the Fonds der Chemischen Industrie.

References

Antao,V.P. and Tinoco,I., Jr (1992) Thermodynamic parameters for loop formation in RNA and DNA hairpin tetraloops. *Nucleic Acids Res.*, **20**, 819–824.

Antao,V.P., Lai,S.Y. and Tinoco,I., Jr (1991) A thermodynamic study of unusually stable RNA and DNA hairpins. *Nucleic Acids Res.*, **19**, 5901–5905.

Baumstark,T. and Riesner,D. (1995) Only one of four possible secondary structures of the central conserved region of potato spindle tuber viroid is a substrate for processing in a potato nuclear extract. *Nucleic Acids Res.*, **23**, 4246–4254.

Beekwilder,M.J., Nieuwenhuizen,R. and v.Duin, J. (1995) Secondary structure model for the last two domains of single-stranded RNA phage Qβ. *J. Mol. Biol.*, **247**, 903–917.

Berk,A.J. and Sharp,P.A. (1978) Spliced early mRNAs of simian virus 40. *Proc. Natl Acad. Sci. USA*, **75**, 1274–1278.

Branch,A.D. and Robertson,H.D. (1984) A replication cycle for viroids and other small infectious RNAs. *Science*, **223**, 450–455.

Branch,A.D., Robertson,H.D., Greer,C., Gegenheimer,P., Peebles,C. and Abelson,J. (1982) Cell-free circularization of viroid progeny RNA by an RNA ligase from wheat germ. *Science*, **217**, 1147–1149.

Branch,A.D., Benenfeld,B.J. and Robertson,H.D. (1985) Ultraviolet light-induced crosslinking reveals a unique region of local tertiary structure in potato spindle tuber viroid and HeLa 5S RNA. *Proc. Natl Acad. Sci. USA*, **82**, 6590–6594.

Butcher,S.E. and Burke,J.M. (1994a) A photo-cross-linkable tertiary structure motif found in functionally distinct RNA molecules is essential for catalytic function of the hairpin ribozyme. *Biochemistry*, **33**, 992–999.

Butcher,S.E. and Burke,J.M. (1994b) Structure mapping of the hairpin ribozyme: magnesium-dependent folding and evidence for tertiary interactions within the ribozyme-substrate complex. *J. Mol. Biol.*, **244**, 52–63.

Buzayan,J.M., Gerlach,W.L. and Bruening,G., (1986) Nonenzymatic cleavage and ligation of RNAs complementary to a plant virus satellite RNA. *Nature*, **323**, 349–353.

Candresse,T., Diener,T.O. and Owens,R.A. (1990) The role of the viroid central conserved region in cDNA infectivity. *Virology*, **175**, 232–237.

Casey,J. and Davidson,N. (1977) Rates of formation and thermal stability of RNA:DNA and DNA:DNA duplexes at high concentrations of formamide. *Nucleic Acids Res.*, **4**, 1539–1552.

Cate,J.H., Gooding,A.R., Podell,E., Zhou,K., Golden,B.L., Kundrot,C.E., Cech,T.R. and Doudna,J.A. (1996) Crystal structure of a group I ribozyme domain: principles of RNA packing. *Science*, **273**, 1678–1685.

Chanfreau,G. and Jacquier,A. (1996) An RNA conformational change between the two chemical steps of group II self-splicing. *EMBO J.*, **15**, 3466–3476.

Chen,X., Baumstark,T., Steger,G. and Riesner,D. (1995) High resolution SSCP by optimization of the temperature by TGGE. *Nucleic Acids Res.*, **23**, 4524–4525.

Costa,M. and Michel,F. (1995) Frequent use of the same tertiary motif by self-folding RNAs. *EMBO J.*, **14**, 1276–1285.

Coutts,S.M. (1971) Thermodynamics and kinetics of G:C base pairing in the isolated extra arm of serine-specific transfer RNA from yeast. *Biochim. Biophys. Acta*, **232**, 94–106.

Daròs,J.A., Marcos,J.F., Hernández,C. and Flores,R. (1994) Replication of avocado sunblotch viroid: evidence for a symmetric pathway with two rolling circles and hammerhead ribozyme processing. *Proc. Natl Acad. Sci. USA*, **91**, 12813–12817.

Diener,T.O. (1986) Viroid processing: a model involving the central conserved region and hairpin I. *Proc. Natl Acad. Sci. USA*, **83**, 58–62.

Diener,T.O. (ed.) (1987) *The Viroids*. Plenum Publishing Corporation, New York.

Diener,T.O. (1989) Circular RNAs: Relics of precellular evolution? *Proc. Natl Acad. Sci. USA*, **86**, 9370–9374.

Dinter-Gottlieb,G. (1986) Viroids and virusoids are related to group I introns. *Proc. Natl Acad. Sci. USA*, **83**, 6250–6254.

Etscheid,M., Tousignant,M.E. and Kaper,J.M. (1995) Small satellite of arabis mosaic virus: autolytic processing of *in vitro* transcripts of (+) and (−) polarity and infectivity of (+) strand transcripts. *J. Gen. Virol.*, **76**, 271–282.

Felden,B., Florentz,C., Giegé,R. and Westhof,E. (1994) Solution structure of the 3′-end of brome mosaic virus genomic RNAs: conformational mimicry with canonical tRNAs. *J. Mol. Biol.*, **235**, 508–531.

Forster,A.C. and Symons,R.H. (1987) Self-cleavage of plus and minus RNAs of a virusoid and a structural model for the active sites. *Cell*, **49**, 211–220.

Groebe,D.R. and Uhlenbeck,O.C. (1988) Characterization of RNA hairpin loop stability. *Nucleic Acids Res.*, **16**, 11725–11735.

Groeneveld,H., Thimon,K. and v.Duin,J. (1995) Translational control of maturation-protein synthesis in phage MS2: a role for the kinetics of RNA folding? *RNA*, **1**, 79–88.

Gross,H.J., Domdey,H., Lossow,Ch., Jank,P., Raba,M., Alberty,H. and Sänger,H.L. (1978) Nucleotide sequence and secondary structure of potato spindle tuber viroid. *Nature*, **273**, 203–208.

Gutell,R.R., Schnare,M. and Gray,M. (1992) A compilation of large subunit (23S- and 28S-like) ribosomal RNA structures. *Nucleic Acids Res.*, **20** (suppl.), 2095–2109.

Hashimoto,J. and Machida,Y. (1985) The sequence in the potato spindle tuber viroid required for its cDNA to be infective: a putative processing site in viroid replication. *J. Gen. Appl. Microbiol.*, **31**, 551–561.

Hecker,R., Wang,Z., Steger,G. and Riesner,D. (1988) Analysis of RNA structures by temperature-gradient gel electrophoresis: viroid replication and processing. *Gene*, **72**, 59–74.

Hernández,C. and Flores,R. (1992) Plus and minus RNAs of peach latent mosaic viroid self-cleave *in vitro* via hammerhead structures. *Proc. Natl Acad. Sci. USA*, **89**, 3711–3715.

Hutchins,C.J., Rathjen,P.D., Forster,A.C. and Symons,R.H. (1986) Self-cleavage of plus and minus RNA transcripts of avocado sunblotch viroid. *Nucleic Acids Res.*, **14**, 3627–3640.

Jaeger,L., Michel,F. and Westhof,E. (1994) Involvement of a GNRA tetraloop in long-range RNA tertiary interactions. *J. Mol. Biol.*, **236**, 1271–1276.

Kikuchi,Y., Tyc,K., Filipowicz,W., Sänger,H.L. and Gross,H.J. (1982) Circularization of linear viroid RNA via 2′-phosphomonoester, 3′, 5′-phosphodiester bonds by a novel type of RNA ligase from wheat germ and *Chlamydomonas. Nucleic Acids Res.*, **10**, 7521–7529.

Konarska,M., Filipowicz,W., Domdey,H. and Gross,H.J. (1981) Formation of a 2′-phosphomonoester, 3′, 5′-phosphodiester linkage by a novel RNA ligase in wheat germ. *Nature*, **293**, 112–116.

Krupp,G. (1988) RNA synthesis: strategies for the use of bacteriophage RNA polymerases. *Gene*, **72**, 75–89.

Lafontaine,D., Beaudry,D., Marquis,P. and Perreault,J.-P. (1995) Intra- and intermolecular nonenzymatic ligations occur within transcripts derived form the peach latent mosaic viroid. *Virology*, **212**, 705–709.

Langowski,J., Henco,K., Riesner,D. and Sänger,H.L. (1978) Common structural features of different viroids: serial arrangement of double helical sections and internal loops. *Nucleic Acids Res.*, **5**, 1589–1610.

Loss,P., Schmitz,M., Steger,G. and Riesner,D. (1991) Formation of a thermodynamically metastable structure containing hairpin II is critical for infectivity of potato spindle tuber viroid RNA. *EMBO J.*, **10**, 719–727.

Ma,C.K., Kolesnikow,T., Rayner,J.C., Simons,E.L., Yim,H. and Simons,R.W. (1994) Control of translation by mRNA secondary structure: the importance of the kinetics of structure formation. *Mol. Microbiol.*, **14**, 1033–1047.

Martínez-Soriano,J.P., Galindo-Alonso,J., Maroon,C.J.M., Yucel,I., Smith,D.R. and Diener,T.O. (1996) Mexican papita viroid: putative ancestor of crop viroids. *Proc. Natl Acad. Sci. USA*, **93**, 9397–9401.

Meshi,R., Ishikawa,M., Watanabe,Y., Yamaya,J., Okada,Y., Sano,T. and Shikata,E. (1985) The sequence necessary for the infectivity of hop stunt viroid cDNA clones. *Mol. Gen. Genet.*, **200**, 199–206.

Michel,F. and Dujon,B. (1983) Conservation of RNA secondary structure in two intron families including mitochondrial-, chloroplast- and nuclear-encoded members. *EMBO J.*, **2**, 33–38.

Michel,F. and Westhof,E. (1990) Modelling of the three-dimensional architecture of group I catalytic introns based on comparative sequence analysis. *J. Mol. Biol.*, **216**, 585–610.

Murphy,F.L. and Cech,T.R. (1994) GAAA tetraloop and conserved bulge stabilize tertiary structure of a group I intron domain. *J. Mol. Biol.*, **236**, 49–63.

Paul,C.P., Levine,B.J., Robertson,H.D. and Branch,A.D. (1992) Transcripts of the viroid central conserved region contain the local tertiary structural element found in full-length viroid. *FEBS Lett.*, **305**, 9–14.

Petersen,I., Ohgaki,H., Ludeke,B. and Kleihues,P. (1994) Direct DNA sequencing following SSCP analysis. *Anal. Biochem.*, **218**, 478–479.

Pley,H.W., Flaherty,K.M. and McKay,D.B. (1994) Model for an RNA tertiary interaction from the structure of an intermolecular complex between a GAAA tetraloop and an RNA helix. *Nature*, **372**, 111–113.

Rakowski,A.G. and Symons,R.H. (1994) Infectivity of linear monomeric transcripts of citrus exocortis viroid: terminal sequence requirements for processing. *Virology*, **203**, 328–335.

Riesner,D. and Gross,H.J. (1985) Viroids. *Annu. Rev. Biochem.*, **54**, 531–564.

Riesner,D. and Römer,R. (1973) Thermodynamics and kinetics of conformational transitions in oligonucleotides and tRNA. In Duchesne, J. (ed.), *Physico-chemical Properties of Nucleic Acids.* Academic Press, London, UK, Vol. 2, pp. 237–318.

Riesner,D. and Steger,G. (1990) Viroids and viroid-like RNAs. In Saenger, W. (ed.), *Landolt-Börnstein, New Series, VII Biophysics.* Springer Verlag, Berlin, Germany, Vol. 1, Subvol. d, pp. 194–243.

Sänger,H.L. (1987) Viroid function: viroid replication. In Diener, T.O. (ed.), *The Viroids.* Plenum Publishing Corporation, New York, pp. 117–166.

Schmitz,M. and Steger,G. (1992) Base-pair probability profiles of RNA secondary structures. *Comput. Applic. Biosci.*, **8**, 389–399.

Semancik,J.S. (ed.) (1987) *Viroids and Viroid-like Pathogens.* CRC Press, Boca Raton, FL.

Shen,L.X., Cai,Z. and Tinoco,I., Jr (1995) RNA structure at high resolution. *FASEB J.*, **9**, 1023–1033.

Steger,G. (1994) Thermal denaturation of double-stranded nucleic acids: prediction of temperatures critical for gradient gel electrophoresis and polymerase chain reaction. *Nucleic Acids Res.*, **22**, 2760–2768.

Steger,G., Tabler,M., Brüggemann,W., Colpan,M., Klotz,G., Sänger, H.-L. and Riesner, D. (1986) Structure of viroid replicative intermediates: physico-chemical studies on SP6 transcripts of cloned oligomeric potato spindle tuber viroid. *Nucleic Acids Res.*, **14**, 9613–9630.

Steger,G., Baumstark,T., Mörchen,M., Tabler,M., Tsagris,M., Sänger,H.L. and Riesner, D. (1992) Structural requirements for viroid processing by RNase T1. *J. Mol. Biol.*, **227**, 719–737.

Symons,R.H. (ed.), (1990) Viroids and related pathogenic RNAs. *Semin. Virol.*, **1**.

Szewczak,A.A. and Moore,P.B. (1995) The sarcin/ricin loop, a modular RNA. *J. Mol. Biol.*, **247**, 81–98.

Tabler,M. and Sänger,H.L. (1984) Cloned single- and double-stranded DNA copies of potato spindle tuber viroid (PSTV) RNA and coinoculated subgenomic DNA fragments are infectious. *EMBO J.*, **3**, 3055–3062.

Tsagris,M., Tabler,M. and Sänger,H.L. (1987) Oligomeric potato spindle tuber viroid (PSTV) RNA does not process autocatalytically under conditions where other RNAs do. *Virology*, **157**, 227–231.

Varani,G., Cheong,C. and Tinoco,I., Jr (1991) Structure of an unusually stable RNA hairpin. *Biochemistry*, **30**, 3280–3289.

Wassenegger,M., Spieker,R.L., Tahlmeir,S., Gast,F.-U., Riedel,L. and Sänger,H.L. (1997) A single nucleotide substitution converts potato spindle tuber viroid (PSTVd) from a noninfectious to an infectious RNA for *Nicotiana tabacum. Virology*, in press.

Wimberly,B., Varani,G. and Tinoco,I., Jr (1993) The conformation of loop E of eukaryotic 5S ribosomal RNA. *Biochemistry*, **32**, 1078–1087.

Received on July 8, 1996; revised on October 4, 1996